# A Model of a Closed Cycle of Water Splitting Using *ansa*-Titanocene(III/IV) Triflate Complexes

Christian Godemann, Dirk Hollmann,* Monty Kessler, Haijun Jiao, Anke Spannenberg, Angelika Brückner,* and Torsten Beweries*

Leibniz-Institut für Katalyse e.V. an der Universität Rostock, Albert-Einstein-Strasse 29a, 18059 Rostock, Germany

S *Supporting Information*

ABSTRACT: A series of *ansa*-titanocene triflate complexes are described as model compounds for the elementary steps of light-driven overall water splitting. Titanocene(III) triflate complexes are readily obtained by reaction of a titanocene source with $Yb(OTf)_3$. Subsequent reactions with water and with/without TEMPO as hydrogen scavenger are studied. The as-obtained titanocene(IV) compounds can be photoreduced to give titanocene(III) triflate complexes, which can undergo further hydrolysis to form a closed catalytic cycle of water splitting. No further degradation of the photoreduced species was observed because of the presence of the OTf group. The stability of the system was evaluated in an experiment with high concentrations of water and TEMPO. X-ray crystallography on all titanocene complexes, EPR and NMR spectroscopy, and DFT were used to support our observations.
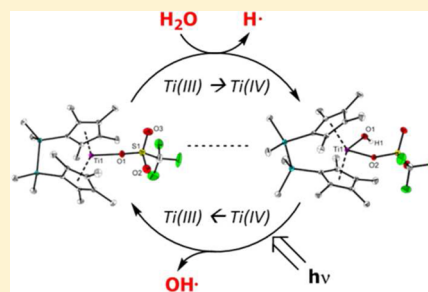
INTRODUCTION

In recent years, water activation and splitting to generate H_2 and O_2 are discussed as a promising way to provide a sustainable and environmentally benign route for the production of a "green" fuel.[1] Numerous reported systems describe light-driven water reduction and oxidation as well as combinations of both half reactions; this is an approach that is often referred to as "artificial photosynthesis".[2] Despite the enormous amount of knowledge being created by optimization of catalyst systems as well as by photophysical and photochemical studies, relatively little is known about the elementary steps of water activation at a transition metal center. This can be rationalized by considering the O−H bond dissociation energy of 499 kJ·mol^{-1}, which is among the highest values for X−H bonds.[3] Additionally, in reaction systems containing water and a low-valent transition metal fragment, depending on the organometallic environment, multiple reaction pathways are possible, which often results in the formation of ill-defined product mixtures.[4] For early transition metal complexes, no well-defined products from oxidative addition reactions are known to date. A reason for this is found to be the limited stability of the in situ formed hydrido-hydroxido compounds, which tend to undergo further conversions to give more stable species.[5]

Thus, to the best of our knowledge, only two systems based on transition metal complexes are known that can mimic both water reduction and water oxidation to give a closed stoichiometric model for a catalytic cycle. Milstein and co-workers described a ruthenium pincer system, in which the PNN ligand is noninnocent and cooperates in the activation of the water molecule to give H_2 and after irradiation O_2.[6] Studies on another organometallic system that is in principle capable of performing both half reactions were published by Kunkely and Vogler, who reported on osmocene complexes that can consecutively produce H_2 and O_2 from water; however, in this case no fully closed synthesis cycle was realized.[7] In our group, we have demonstrated that stepwise selective water reduction takes place at decamethyltitanocene(III) triflate complexes.[8] The mechanism of this reaction was elucidated by in situ FTIR and EPR spectroscopy as well as DFT computation.[9] As a model for the second half reaction (i.e., water oxidation), photolysis of a decamethyltitanocene(IV) dihydroxido complex gave the photoreduced monohydroxido species by Ti−O bond activation. However, as the main reaction pathway, elimination of a cyclopentadienyl ligand was observed, thus preventing the determination of OH radicals.[10] This led to the formation of tetranuclear Ti(IV) side products that could not be transferred into a species that would be of importance for a sequence involving reactions of Ti(III)/(IV) species and water. Recently, exclusive Ti−O bond activation to yield a singly reduced Ti(III) monohydroxido compound was observed in the photolysis of structurally similar *ansa*-titanocenes.[11,12] Here no cyclopentadienyl ligand dissociation was detected. Isolation and full characterization of the organometallic photolysis product was not possible because the produced Ti(III) complex underwent condensation to yield oxido-bridged titanocene compounds. To combine the benefits of (a) selective and stepwise hydrolysis of Ti(III) triflate complexes and (b) the photostability of the *ansa*-metallocene unit, we aimed for the preparation of *ansa*-titanocene(III) complexes with triflate as stabilizing ligand.

In this contribution, we present an *ansa*-titanocene(III/IV) system that is capable of formally performing both water reduction (by oxidation of a Ti(III) species) as well as water oxidation (by photoreduction of a Ti(IV) complex), thus resulting in a closed catalytic cycle for overall water splitting.

■ RESULTS AND DISCUSSION

Synthesis of an *ansa*-Titanocene(III) Triflate Complex. Synthesis of the disila-bridged fully methylated titanocene(III) triflate complex was performed via the preparation procedure reported earlier for a similar decamethyltitanocene complex.[8] Starting from titanocene precursor **1**, oxidation with Yb(OTf)$_3$ gives the corresponding triflate complex **2** as a green solid in good yield (Scheme 1). It should be noted that selective introduction of the triflate group using Fe(OTf)$_3$ as described before[8] was not successful.

**Scheme 1. Synthesis of Titanocene(III) Triflate Complex 2**
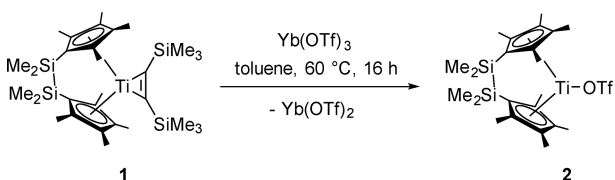
Single crystals of complex **2** suitable for X-ray analysis were obtained from saturated toluene solutions at 20 °C. The molecular structure is depicted in Figure 1. It shows the typical
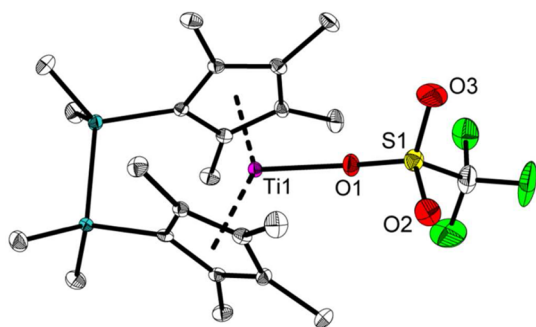
Figure 1. Molecular structure of complex **2**. Thermal ellipsoids correspond to 30% probability. Hydrogen atoms are omitted for clarity.

bent bridged titanocene fragment and the triflate group being κ^1-*O*-coordinated to the central Ti atom. Structural parameters are very similar to those found before for the unbridged complex Cp*$_2$Ti(OTf) (e.g., **2**: Ti−O 2.066(2); Cp*$_2$Ti(OTf): Ti−O 2.078(1) Å).

EPR spectra of compound **2** were recorded in toluene (Figure 2). Careful analysis reveals the presence of three different species of **2** indicated as **2-I** (Figure 2c), **2-II** (Figure 2d), and **2-III** (Figure 2e). We believe that the coordinated triflate ligand in complex **2** interacts with further Ti(III) complexes because in highly diluted solution signal **2-III** disappears and only signal **2-I** was observed. The resulting magnetic interaction between the paramagnetic centers causes the line broadening in **2-III**. Note that the signal intensities strongly depend on the concentration of complex **2** (Figure S1). This was reported before for the unbridged decamethyltitanocene(III) triflate complexes.[9]
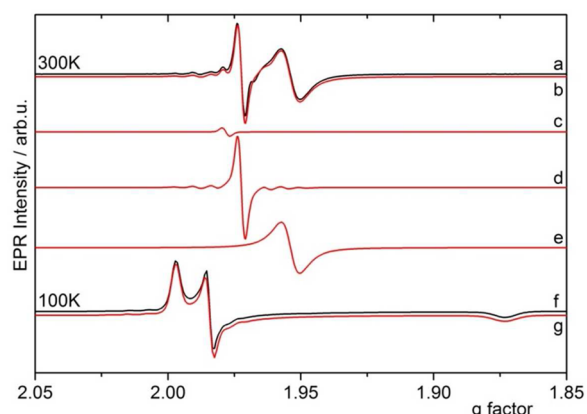

Figure 2. EPR spectra of complex **2** in toluene. (a and f) Experimental spectra at 300 and 100 K, respectively; (b) 300 K simulated spectrum[14] comprising contributions from (c) species **2-I** (g = 1.9784, A$_{Ti}$ = n.d, ΔB = 5.0 G, contribution 3%), (d) **2-II** (g = 1.9726, A$_{Ti}$ = 11.5 G, ΔB = 5.0 G, contribution 39%), and (e) **2-III** (g = 1.9541, A$_{Ti}$ = n.d., ΔB = 12.3 G, contribution 58%); (g) 100 K: simulated spectrum (g_1 = 1.9972, A$_{Ti}$ = 11.5 G, ΔB$_1$ = 5.5 G, g_2 = 1.9842, ΔB$_2$ = 4.2 G, g_3 = 1.8736, ΔB$_3$ = 16 G).

Signal **2-II** shows typical hyperfine structure (hfs) splitting resulting from the coupling of the single electron of Ti^{III} to the nuclear spin of the isotopes ^{47}Ti (I = $^5/_2$, 7.44% natural abundance) and ^{49}Ti (I = $^7/_2$, 5.41% natural abundance). This is characteristic for isolated Cp*$_2$Ti^{III}OR complexes.[13] The spectrum of the frozen solution at 100 K contains only one single rhombic signal, which reflects all Ti(III) species in the sample and clearly shows that the direct environment of each Ti(III) is the same (Figure 2f).

Reaction of *ansa*-Titanocene Triflate Complexes with Water. As a model for the first half reaction of overall water splitting, we investigated the reaction of complex **2** with water. Here, a rapid color change and precipitation of blue to greenish material indicated the formation of the hydrolysis product (Scheme 2). NMR spectroscopy showed very broad resonances

Scheme 2. Reaction of Complex 2 with Water
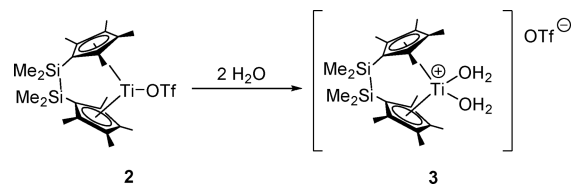
that suggest the presence of a paramagnetic species. To understand the observed reactivity and stabilities of these complexes, we carried out density functional theory computation using the range-separated hybrid WB97XD functional that includes dispersion correction.[15] This method has been found increasingly important in describing ligand effects.[16] The computational details are given in the Supporting Information. The results show that hydrolysis of complex **2** with an excess of water to give **3** is thermodynamically favored by 7.38 kcal/mol.

Fortunately, suitable single-crystalline samples of complex **3** for the determination of its molecular structure (Figure 3) could be obtained by diffusion of *n*-hexane into a THF solution at room temperature. Compared to the starting material, the triflate group was substituted by two aqua ligands and is now found in the secondary coordination sphere. Ti−O bond
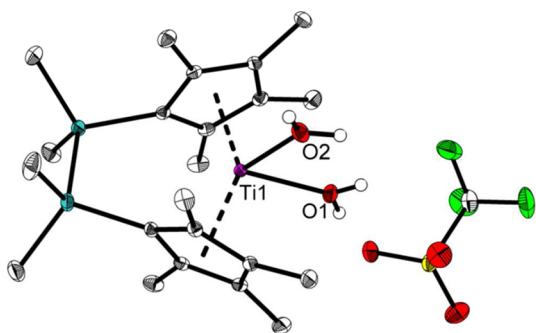
Figure 3. Molecular structure of complex **3**. Thermal ellipsoids correspond to 30% probability. Hydrogen atoms (except those bound to O1 and O2) and the solvent molecule (THF) are omitted for clarity.

lengths are in the typical range for titanocene diaqua complexes (Ti1−O1 2.1341(11), Ti1−O2 2.1615(11) Å). However, compared to the similar Ti(IV) complex $[Cp*_2Ti(H_2O)_2]$-$(OTf)_2$ described by Thewalt and Honold (2.062(6) and 2.089(6) Å),[17] the Ti−O contacts in **3** are slightly longer, most likely because of the higher electron density at the Ti(III) center. Furthermore, as in $[Cp*_2Ti(H_2O)_2](OTf)_2$, hydrogen bonding to the OTf ligand was observed with an additional interaction to THF in the herein described complex **3** (Figure S5). For the unbridged complex $[Cp*_2Ti(H_2O)_2](OTf)$, DFT calculations implied that this should be of importance for the subsequent formation of H_2 and oxidation of the Ti(III) center.[9]

EPR spectra of complex **3** were recorded in THF solution (Figure 4). At room temperature, a single line of an isolated
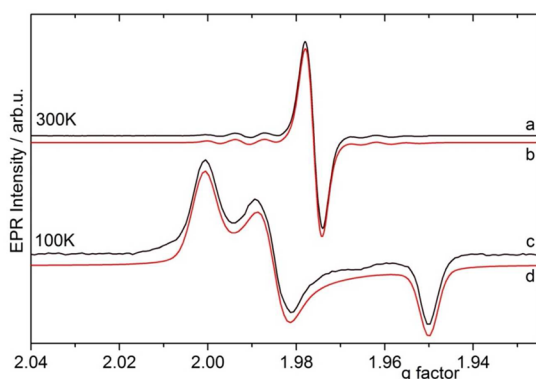
Figure 4. Experimental (black) and simulated[14] EPR spectra (red) of complex **3** in toluene. Spin Hamiltonian parameters: (b) 300 K: g = 1.9770, A_{Ti} = 11.0 G, ΔB = 5.6 G; (d) 100 K: g_1 = 2.009, ΔB_1 = 8.7 G, g_2 = 1.9852, ΔB_2 = 9.4 G, g_3 = 1.9503, ΔB_3 = 7.0 G).

Ti(III) center with the typical hfs was detected. Notably, the experimental spectrum showed an additional but not well-resolved splitting that may stem from superhyperfine structure (shfs) coupling to hydrogen (identified in the third derivative, Figure S2). Such shfs with a similar coupling constant has also been observed upon treatment of $[Cp*_2Ti^{III}(OTf)]$ with water.[9] Unfortunately at room temperature **3** has nearly the same g factor (g = 1.9770) as **2-II** (g = 1.9726). Here only the low-temperature measurements can clearly distinguish between **3** and **2**. (Compare Figures 2g and 4d.)

Chemical Oxidation of the Ti(III) Center. Interestingly, the diaqua complex **3** is rather stable at room temperature.

Even at elevated temperature only very slow oxidation to the corresponding Ti(IV) complex was observed on a preparative scale. This is in strong contrast to the unbridged complex $Cp*_2Ti(OTf)$ reported before, for which the formed $[Cp*_2Ti-(H_2O)_2](OTf)$ complex is not stable and releases hydrogen even at room temperature. However, in the presence of excess water, after formation of **3**, this species is oxidized to an EPR inactive Ti(IV) complex. This can be seen from Figure 5, which shows time-dependent EPR spectra of a THF solution of complex **2** in the presence of water leading first to the formation of **3** and subsequently to its decay.
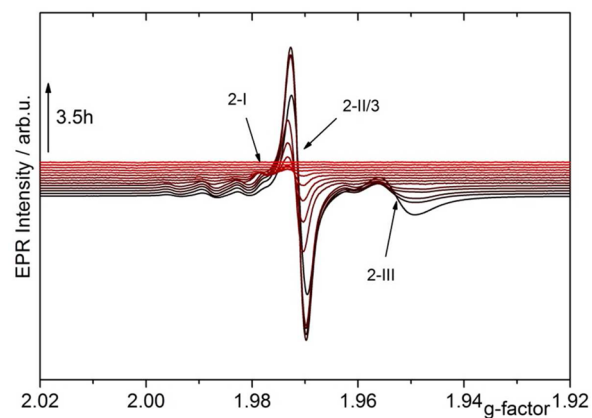

Figure 5. Time-resolved EPR measurements of complex **2** after addition of a water/THF mixture. (Selected spectra of this experiment are shown in Figure S3.)

To accelerate the hydrogen abstraction process of **3**, we added (2,2,6,6-tetramethyl-piperidin-1-yl)oxyl (TEMPO) as a hydrogen radical scavenger. In this case, fast abstraction of a hydrogen atom and oxidation of the Ti(III) center was observed to give the diamagnetic complex **4** (Scheme 3).

Upon addition of a TEMPO solution to a suspension of complex **3** (both in toluene), immediate color change from greenish-blue to red was observed. ¹H NMR analysis of the reaction mixture revealed the formation of a diamagnetic titanocene species along with the evolution of broad resonances at 1.08 and 1.38 ppm in toluene-d_8 that can be assigned to the methyl groups and ring protons of the resulting TEMPO−H compound (Figures S7 and S8). The characteristic N−OH signal could not be observed at room temperature because of fast proton exchange.[18] A broad resonance could however be detected at 6.07 ppm upon cooling to 203 K (Figure S9). Note that this value is different compared to that observed before for neat TEMPO−H in benzene-d_6,[19] most likely because of hydrogen bonding being present to complex **4**. For the cyclopentadienyl methyl and dimethylsilyl groups of titanocene species **4**, only three resonances could be observed, which indicates a symmetric coordination sphere in solution due to fluxionality between one proton of the aqua ligand and the OH ligand. Therefore, instead of an isolated resonance for the OH ligand, only a broad resonance corresponding to three protons could be observed. Upon cooling to 203 K, this resonance is split into two isolated singlets, which allows for the determination of an activation barrier of this fluxional process of 8.44 kcal/mol (Figure S10). Also, EPR spectra show an immediate quench of the paramagnetic Ti(III) resonance after addition of TEMPO. DFT analysis shows this oxidation and

Scheme 3. Oxidation of the Ti(III) Center and Removal of Water
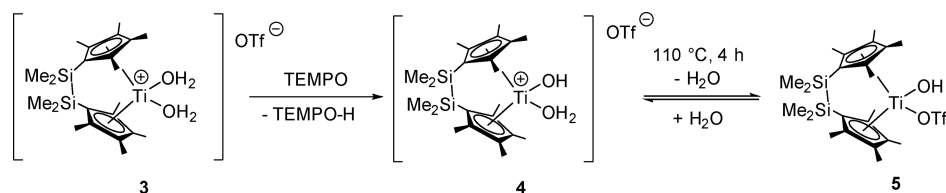
abstraction of a hydrogen radical to be an exergonic step ($\Delta G = -2.81$ kcal/mol).

NMR spectroscopic monitoring of the hydrolysis of complex **2** using D_2O, followed by oxidation of the corresponding deuterated Ti(III) product **3**, showed the absence of the above-mentioned broad H_2O/OH signal along with a fully intact set of resonances corresponding to ligand methyl groups (Figure S11). This confirms that the hydrogen radical is selectively abstracted from one of the introduced aqua ligands and not from the bridged cyclopentadienyl ligand.

Single crystals suitable for an X-ray analysis were obtained by slow diffusion of air into an NMR tube containing a toluene-d_8 solution of complex **3**. The molecular structure of ionic complex **4** shows the titanium atom being surrounded by the *ansa*-Cp′ ligand, the OH group, and the aqua ligand in a distorted tetrahedral coordination geometry (Figure 6).
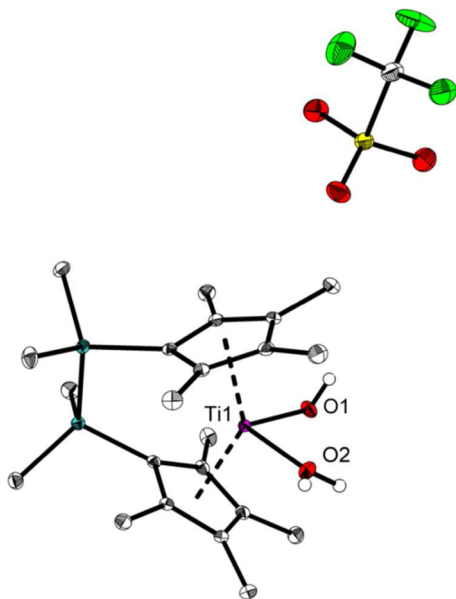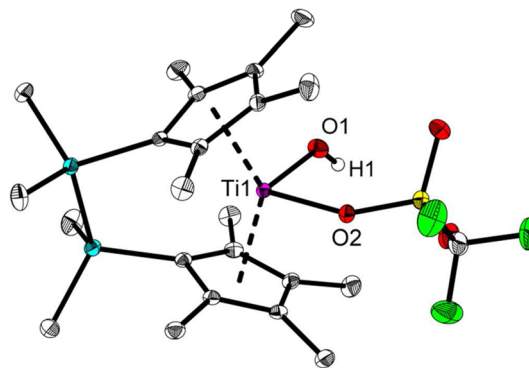

Figure 6. Molecular structure of complex **4**. Thermal ellipsoids correspond to 30% probability. Hydrogen atoms (except those bound to O1 and O2) are omitted for clarity.

Similarly as in complex **3**, the triflate group is located in the secondary coordination environment, but in this case, no direct hydrogen bridges to any of the protons of the Ti(H$_2$O)(OH) moiety were observed. Instead, cocrystallized water occupies the interionic space in the solid state and builds a hydrogen bonding network between the triflate anion and the titanocene fragment (Figure S6). The different nature of the oxygen containing ligands can be derived from a comparison of the Ti−O bond lengths (Ti1−O1 1.9072(12) Å and Ti1−O2 2.0548(13) Å), with the longer bond being characteristic for Ti aqua complexes complex **3**. These are in the same range as those found for complexes displaying a very similar cationic

fragment that were described before by Bochmann and co-workers[20] and Thewalt and Honold.[17]

Removal of the remaining aqua ligand from complex **4** is computed to be exergonic ($\Delta G = -4.02$ kcal/mol) and was possible by heating solid samples to 110 °C under vacuum for several hours (Scheme 3). It should be noted that this process is reversible because **4** is reformed in the presence of water. The neutral complex **5** could be obtained in good yields as a red powder by recrystallization from toluene to give analytically pure material. The ^{1}H NMR spectrum (Figure S13) shows six resonances due to the methyl groups ($2 \times SiMe_2$, $4 \times C_5Me_4$) of the bridging ligand, thus indicating an asymmetry in solution. A singlet corresponding to the OH group was detected in the downfield region at 10.62 ppm. This is well in line with the value found before for the similar complex Cp*$_2$Ti(OH)(OTf) (δ(OH) 10.41 ppm).[8]

In the molecular structure of complex **5** (Figure 7), the Ti center adopts the typical distorted tetrahedral coordination


Figure 7. Molecular structure of complex **5**. Thermal ellipsoids correspond to 30% probability. Hydrogen atoms (except H1) are omitted for clarity.

geometry, which is well-known for titanocene(IV) compounds. The bonding distance Ti1−O1 of 1.866(2) Å is in the expected range and is slightly shorter than the value determined for Cp*$_2$Ti(OH) (OTf) (1.884(2) Å).[8]

Photolysis of the Ti(IV) Complexes 4 and 5. On the basis of our studies of the photochemical Ti−O bond activation using neutral titanocene(IV) dihydroxido species,[12] we assumed that structurally similar complexes **5** and/or **4** display the same reactivity. The reported photochemical metal−oxygen bond activation could be described as a model for the second half reaction of overall water splitting.

Photolysis of **4** and **5** was monitored by in situ EPR spectroscopy. First, the isolated complex **4** was dissolved in toluene and subsequently irradiated with visible light using a 300 W Xe arc lamp (420 nm cutoff filter). As can be seen from Figure 8a, all three species of complex **2** (Figure 2) are formed with time. Note that because of coordinated water being present in **4** the formation of **3** cannot be excluded. The same
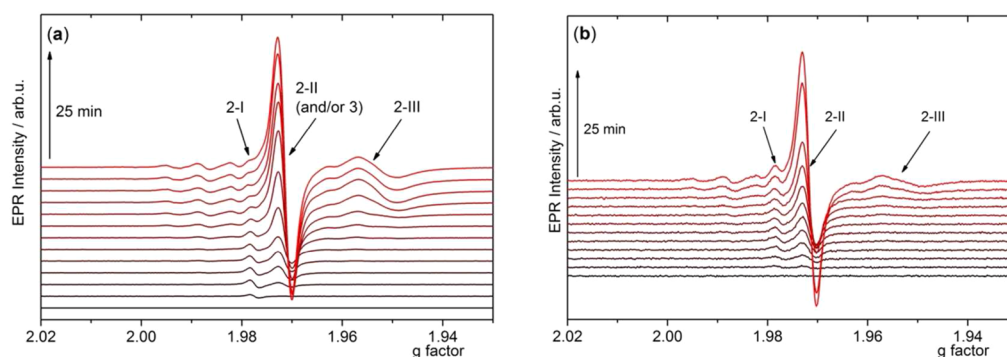
Figure 8. Time-resolved EPR spectra of (a) complex **4** (in toluene) and (b) complex **5** (in benzene) under irradiation with visible light.

Scheme 4. Irradiation of Complexes 4 and 5 Resulting in the Formation of 2[a]
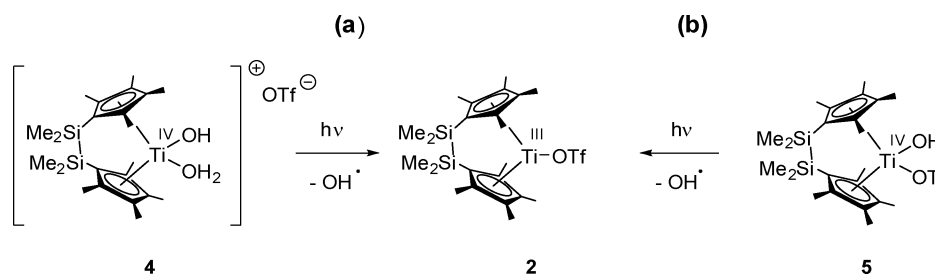
[a]See corresponding EPR spectra in Figure 8.

behavior was observed during the irradiation of **5** (Figures 8b and S4). For complex **5**, this conversion is highly endergonic (ΔG = 64.87 kcal/mol); thus, irradiation with UV or visible light is needed. In both cases, selective Ti−OH bond splitting occurs (Scheme 4). Because the photolysis was performed in the absence of water, no further reaction to **3** proceeds.

When the photolysis reaction of **4** was performed in the presence of an excess of water (1.4% water in methyl-*tert*-butyl ether, MTBE), only a single EPR signal was observed (Figure 9). All EPR parameters (*g* value, hfs to Ti) confirm the
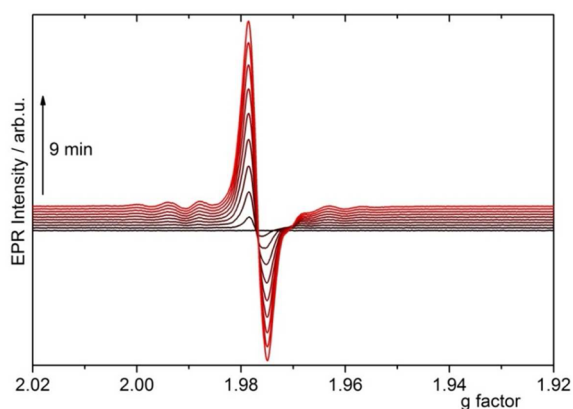

Figure 9. Time-resolved EPR spectra of complex **4** in MTBE−water solution (1.4% water) under irradiation with UV−vis light.

formation of the diaqua complex **3** (Scheme 5). Thus, both in the presence and absence of water, the Ti(IV) center is photoreduced to give Ti(III) complexes with activation of the Ti−OH bond.

Attempts to trap the formed OH radicals using 5-(diethoxyphosphoryl)-5-methyl-1-pyrroline-*N*-oxide (DEPM-

**Scheme 5. Photolysis of Complex 4 in the Presence of an Excess of Water**[a]
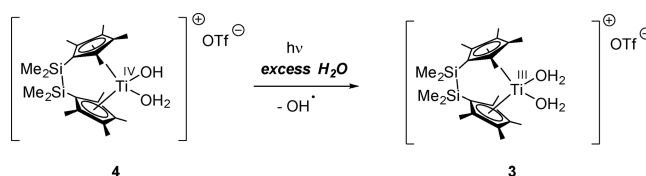
[a]See corresponding EPR spectra in Figure 9.

PO) or 5,5-dimethyl-1-pyrroline-*N*-oxide (DMPO) were not successful because the formation of alkyl adducts with the spin-trapping agents was the only observed reaction (see ref 12's Supporting Information). Unfortunately, different from our previous observations for a similar *ansa*-titanocene dihydroxido complex, addition of the cyclic biradicaloid species [PN(Ter)]$_2$ (Ter = 2,6-Mes$_2$-C$_6$H$_3$; Mes = 2,4,6-Me$_3$C$_6$H$_2$) to trap the OH radicals as a P(III)−OH adduct failed as well because no conversion of the biradicaloid was observed in ^{31}P NMR spectra.

Model of a Closed Cycle of Overall Water Splitting at Ti(III/IV) Centers. To investigate a complete catalytic cycle (Scheme 6), reactions with an excess of water and TEMPO as hydrogen radical scavenger were performed and monitored by NMR and EPR spectroscopy. First, a diluted solution of complex **4** (1.7 mM in THF/water 2%) and a small amount of TEMPO (ratio of TEMPO/**4** = 0.048) was irradiated with UV−vis light to demonstrate the reaction principle by means of in situ EPR spectroscopy. UV−vis light was used because the reaction in the presence of visible light was only very slow. Also, in diluted solutions no line broadening due to dipolar interaction of the Ti(III) centers is observed, thus allowing for a better identification of intermediates. Here the TEMPO resonance was quickly quenched (Figure 10). This indicates a

**Scheme 6. Closed Model Cycle for Overall Water Splitting**
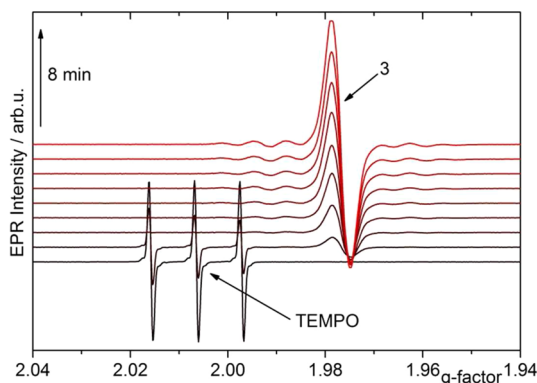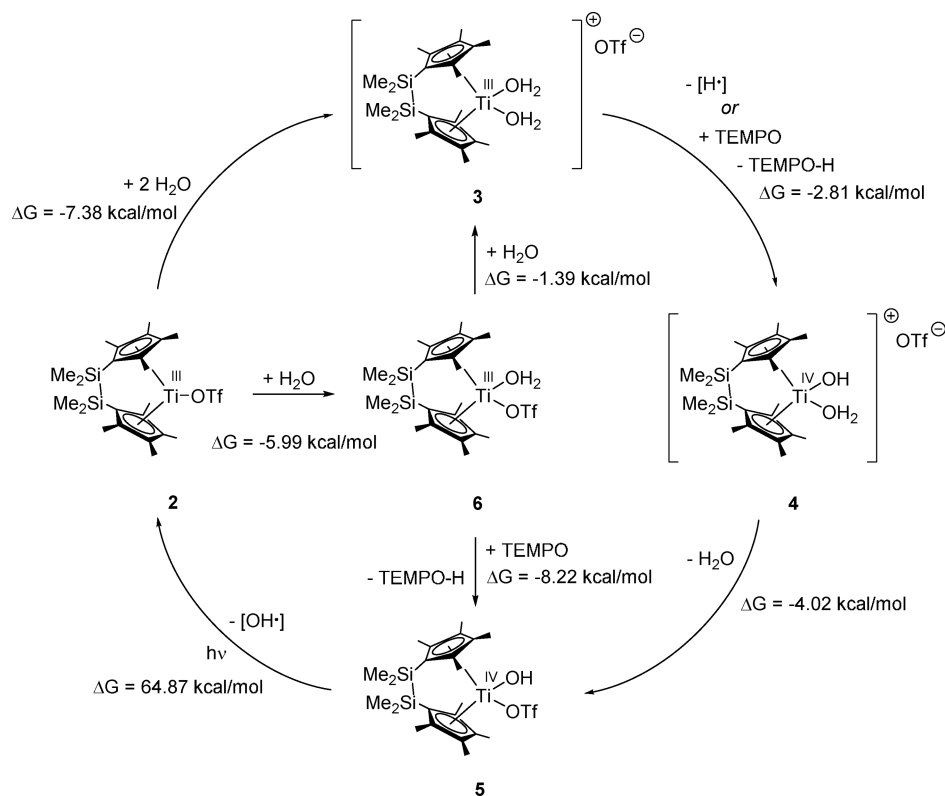
Figure 10. Time-resolved EPR spectra of complex **4** and TEMPO in a THF−water solution (2 vol %) under UV−vis irradiation.

reaction of the Ti(III) complex **3**, formed under irradiation and with an excess of water (Figure 9, Scheme 5), with TEMPO, forming complex **4**. After full consumption of TEMPO, no further oxidation of **3** can occur resulting in an increase of the EPR signal of **3**. The EPR spectrum recorded after immediate cooling to 100 K confirms the presence of the diaqua complex **3** (Figure 4).

To evaluate the possibility of a truly catalytic system, in situ EPR and ex situ NMR measurements of complex **4** (10 mg, 0.0176 mM) with high concentrations of TEMPO (10 mg, 0.0625 mM) and water (20 µL, 0.001 M) in THF were performed. The reaction mixture was monitored by in situ EPR spectroscopy during UV−vis irradiation. NMR runs were performed after 1, 4, and 19 h to quantify the amount of TEMPO−H using benzene as an internal standard. In the beginning, a broad EPR signal of dipolarily interacting TEMPO molecules was detected. However, during irradiation a

continuous narrowing of the TEMPO signal was observed because mutual dipolar interactions are diminished as a result of a decrease of the TEMPO concentration caused by its consumption (Figure 11). Using NMR, a decrease of the
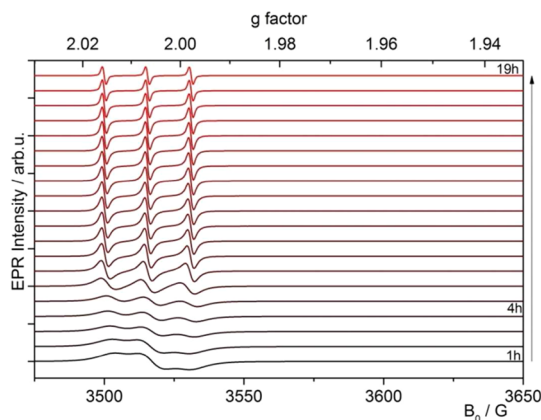
Figure 11. Time-resolved EPR spectra of complex **4** with an excess of TEMPO and water under irradiation with UV−vis light.

water signal as well as an increase of the signal due to the methyl groups of TEMPO−H were detected (Figures S14− S16). Quantification of this conversion in terms of a turnover number was however not possible because of overlapping signals in the ^{1}H NMR spectrum and highly reactive species being present. This supports the photoreduction of complex **4** to **3** and reoxidation of the latter as long as TEMPO is available (Figure 10).

Complex **4** is not stable over a long period of irradiation. By NMR spectroscopy, a clear degradation of the complex is

observed. However, this is not surprising in the presence of large amounts of TEMPO radicals and prolonged UV–vis irradiation with formation of highly reactive OH radicals.

On the basis of the presented results, we postulate a closed model cycle of overall water splitting at a substituted titanocene(III)/(IV) fragment (Scheme 6). It should be noted that as an alternative pathway the reaction of complex **2** with only 1 equiv of water to give unobserved species **6** was computed to be thermodynamically feasible ($\Delta G = -5.99$ kcal/mol). From this, reaction with TEMPO could in principle also give Ti(IV) compound **5**. However, the low barrier for conversion of **6** into **3** suggests that both complexes are in equilibrium with the addition of two equivalents of water being slightly favored.

CONCLUSIONS

In this contribution, we have presented a series of *ansa*-titanocene triflate complexes that can serve as model complexes in a fully closed catalytic cycle of light-driven overall water splitting. Key features for the realization of this are the *ansa*-cyclopentadienyl ligand, which remains coordinated to the metal center,[12] as well as the close proximity of the triflate group, which stabilizes the bonded water molecules and thus helps to prevent further reactions of the formed Ti(III) complexes. In an irradiation experiment using an excess of water and TEMPO as the hydrogen radical scavenger, we have shown that Ti(IV)/Ti(III) photoreduction takes place followed by reoxidation as long as TEMPO is available. This shows that a catalytic reaction is in principle possible; however, further investigations in order to replace TEMPO are needed. To the best of our knowledge, besides the system reported earlier by Milstein and co-workers, this is only the second example for such a model system that contains organometallic species that can be fully interconvertible by oxidation/reduction and concomitant abstraction of hydrogen and hydroxyl radicals.

EXPERIMENTAL DETAILS

General. All manipulations were carried out in an oxygen- and moisture-free argon atmosphere using standard Schlenk and glovebox techniques. All solvents were taken from a solvent purification system (PureSolv, Innovative Technology) or dried over sodium/benzophenone and freshly distilled prior to use. Yb(OTf)$_3$ was purchased from Sigma-Aldrich and used as received. TEMPO was obtained from Sigma-Aldrich (99%) and ABCR (>98%) and used as received. Complex **1** was prepared according to a published procedure.[11] The following instruments were used: NMR: Bruker AV 300. ^{1}H and ^{13}C chemical shifts are given in ppm (δ) and were referenced using the chemical shifts of residual proton solvent resonances: benzene-d_6 (δH 7.16, δC 128.0). EPR: In situ EPR spectra in X-band were recorded by a Bruker EMX CW-micro spectrometer equipped with an ER 4131VT Digital Temperature Control System and an ER 4119HS-WI high-sensitivity optical resonator. The samples were irradiated with a Xe arc lamp (300 W, LOT-Oriel GmbH & Co. KG). The following parameters were used: microwave frequency: 9.4 GHz, microwave power: 6.92 mW, receiver gain: 1×10^3, modulation frequency: 100 kHz, modulation amplitude: 0.4 G, Sweep time: 61.44 s. g factors have been calculated from the resonance field B_0 and the resonance frequency ν using the resonance condition $h\nu = g\beta B_0$. The calibration of the g values was performed using a DPPH standard ($g = 2.0036 \pm 0.00004$). Analysis of the experimental spectra was performed using the simulation program EPRSim32 of Sojka and co-workers.[14] IR (Figures S17–19): Bruker Alpha FT-IR Spectrometer. MS (Figures S20–23): Finnigan MAT 95-XP (Thermo-Electron). Elemental analysis: Leco TruSpec Micro CHNS. Melting points: Büchi 535 apparatus. Melting points are uncorrected and were measured in sealed

capillaries. X-ray analysis: Bruker Kappa APEX II Duo diffractometer. The structures were solved by direct methods and refined by full-matrix least-squares procedures on F^2 with the SHELXTL software package.[21] Diamond was used for graphical representation.[22] CCDC 1429788−1429791 contain the crystallographic data for this paper. These data can be obtained free of charge from The Cambridge Crystallographic Data Center via www.ccdc.cam.ac.uk/data_request/cif.

Synthesis of Complex 2. Complex **1** (0.988 g, 1.72 mmol) and Yb(OTf)$_3$ (1.100 g, 1.77 mmol) were dissolved in 10 mL of toluene resulting in a brownish solution. The mixture was stirred at 60 °C overnight to give a color change to dark green. More toluene was added to dissolve the formed precipitate of the product complex, and the solution was filtered to remove the Yb(OTf)$_2$ residue. Drying under vacuum furnished complex **2** as a dark-green powder. Yield: 0.610 g (1.10 mmol, 64%). C$_{23}$H$_{36}$F$_3$O$_3$SSi$_2$Ti (553.63 g·mol^{-1}). Mp: 110 °C (slow dec.). Anal. Calcd (Found): C = 49.9 (49.82), H = 6.55 (6.61), S = 5.79 (5.87). MS (CI, *iso*-butane): *m/z* 461 [M − OTf + C$_4$H$_9$]$^+$, 420 [M − SO$_2$CF$_3$]+. IR (cm^{-1}): 2952, 2910, 1342, 1335, 1235, 1196, 1173, 827, 787, 764, 741, 630.

Synthesis of Complex 3. Complex **2** (0.100 g, 0.18 mmol) was dissolved in 60 mL of toluene and an excess of water (20 μL, 1.11 mol) was added resulting in a color change from dark-green to light-green/blue and precipitation of small green/blue needles. Decantation of the solvent and drying under vacuum gave complex **3** as a greenish/blue powder. Yield: 0.051 g (48%, 0.09 mmol). C$_{23}$H$_{40}$F$_3$O$_5$SSi$_2$Ti (589.66 g·mol^{-1}). Mp: 130 °C (slow dec.). Anal. Calcd (Found): C = 46.85 (42.59), H = 6.48 (5.89), S = 5.44 (5.29). MS (CI, *iso*-butane): *m/z* 570 [M − H$_2$O − H]$^+$, 553 [M − (2H$_2$O)]$^+$, 420 [M − OTf − H$_2$O − 2H]$^+$, 404 [M − OTf − (2H$_2$O)]$^+$. IR (cm^{-1}): 3398, 2903, 1682, 1634, 1383, 1330, 1247, 1235, 1226, 1170, 1028, 828, 786, 637.

Synthesis/Data of Complex 4. To a suspension of complex **3** (0.075 g, 0.13 mmol) in 10 mL of toluene was added a solution of TEMPO (0.024 g, 0.15 mmol) in 10 mL of toluene. An immediate color change from green/blue to red occurred along with dissolving of all material of complex **3**. Because of the volatile nature of the H$_2$O ligand only NMR values were obtained. NMR: ^{1}H (toluene-d_8, 300 MHz, 298 K, δ) 0.41 (s, 12 H, Si$\underline{Me}_2$), 1.89 (s, 12 H, C$_5\underline{Me}_4$), 1.92 (s, 12 H, C$_5\underline{Me}_4$). ^{1}H (THF-d_8, 300 MHz, 298 K, Figure S12, δ) 0.57 (s, 12 H, Si$\underline{Me}_2$), 1.86 (s, 12 H, C$_5\underline{Me}_4$), 1.99 (s, 12 H, C$_5\underline{Me}_4$). ^{19}F (toluene-d_8, 282.4 MHz, 298 K, δ) −77.30 (s, CF$_3$). MS (CI, *iso*-butane): *m/z* 569 [M − 2H − H$_2$O]$^+$, 439 [M − OTf]$^+$, 420 [M − OTf − H$_2$O]$^+$.

Synthesis of Complex 5. A solution of **4** was filtered, and all volatiles were removed under vacuum, followed by drying of the residue at 110 °C for 4 h to give complex **5** as a red powder. Yield: 0.057 g (76%, 0.10 mmol). C$_{23}$H$_{37}$F$_3$O$_4$SSi$_2$Ti (570.64 g·mol^{-1}). Mp: 120 °C (slow dec.). Anal. Calcd (Found): C = 48.41 (48.15), H = 6.54 (6.36), S = 5.62 (5.57). NMR: ^{1}H (benzene-d_6, 300 MHz, 298 K, δ) 0.29 (s, 6 H, Si$\underline{Me}_2$), 0.40 (s, 6 H, Si$\underline{Me}_2$), 1.64 (s, 6 H, C$_5\underline{Me}_4$), 1.88 (s, 6 H, C$_5\underline{Me}_4$), 1.93 (s, 6 H, C$_5\underline{Me}_4$), 2.06 (s, 6 H, C$_5\underline{Me}_4$), 10.62 (s, 1 H, O$\underline{H}$). ^{19}F (benzene-d_6, 282.4 MHz, 298 K, δ) −75.57 (s, CF$_3$). ^{13}C (benzene-d_6, 100.6 MHz, 298 K, δ) −0.3 (s, Si$\underline{Me}_2$), 0.0 (s, SiMe_2), 8.2 (s, C$_5\underline{Me}_4$), 11.8 (s, C$_5\underline{Me}_4$), 15.0 (s, C$_5\underline{Me}_4$), 15.8 (s, C$_5\underline{Me}_4$), 124.2 (s, $\underline{C}_5$Me$_4$), 124.3 (s, $\underline{C}_5$Me$_4$), 131.1 (s, $\underline{C}_5$Me$_4$), 135.4 (s, $\underline{C}_5$Me$_4$), 143.5 (s, $\underline{C}_5$Me$_4$). ^{29}Si (benzene-d_6, 79.5 MHz, 298 K, δ) −12.44 (SiMe_2). MS (CI, *iso*-butane): *m/z* 569 [M − H]$^+$, 553 [M − OH]$^+$, 439 [M − OTf + H$_2$O]$^+$, 420 [M − OTf − H]$^+$. ATR-IR (32 scans, cm^{-1}): 3647 (w), 2893 (w), 1442 (w), 1406 (w), 1375 (m), 1336 (m), 1251 (m), 1019 (m), 828 (m), 814 (m), 789 (m), 763 (m), 655 (m), 579 (s), 569 (s), 551 (vs), 435 (s).

Experimental Procedures for Irradiation Experiments. Irradiation of complex **4** (Figure 8): A solution of complex **4** (10 mg, 0.017 mmol) in 10 mL of toluene was placed into a J. Young EPR tube in the glovebox, introduced into the EPR spectrometer, and irradiated with an LOT Oriel 300 W Xe lamp. Spectra were recorded at given reaction/irradiation times.

Irradiation of complex **4** in the presence of an excess of water to give **3** (Figure 9): In the glovebox, complex **4** (10 mg, 0.017 mmol) was dissolved in 10 mL of a saturated solution of water in MTBE, and

the solution was placed into a J. Young EPR tube, introduced into the EPR spectrometer, and irradiated with an LOT Oriel 300 W Xe lamp. Spectra were recorded at given reaction/irradiation times.

Irradiation of complex **4** in the presence of water and TEMPO (Figure 10): In the glovebox, complex **4** (10 mg, 0.017 mmol) was dissolved in 10 mL of a solution of water in THF (2 vol %), and TEMPO (0.13 mg, 0.838 μmol) was added. The solution was placed into a J. Young EPR tube, introduced into the EPR spectrometer, and irradiated with an LOT Oriel 300 W Xe lamp. Spectra were recorded at given reaction/irradiation times.

Irradiation of complex **4** in the presence of an excess of water and TEMPO (Figure 11): In the glovebox, complex **4** (10 mg, 0.017 mmol) was dissolved in 10 mL of THF, and water (20 μL, 0.001 mmol) and TEMPO (10 mg, 0.064 mmol) were added. The solution was filled into a J. Young EPR tube, introduced into the EPR spectrometer, and irradiated with an LOT Oriel 300 W Xe lamp. Spectra were recorded at given reaction/irradiation times.

Computational Details. In our calculations, we used all real-size model systems without any simplification or constrains. We employed the BP86[23] functional in combination with the TZVP[24] basis set for all nonmetal elements and LANL2DZ[25] basis set for titanium for the equilibrium geometry optimizations and the subsequent frequency calculations, which characterize the optimized structures as energy minimums without imaginary frequencies. BP86 can give not only reasonable geometries but also the right relative energies for titanocene chemistry.[26] Single-point energy calculations at ωB97XD/TZVP[15] (LAL2DZ basis set for Ti) on the BP86/TZVP optimized geometries for the dispersion correction were carried out. The computed Gibbs free energies (ΔG) at 298 K were calculated from the total electronic energies from ωB97XD/TZVP, and the thermal corrections deduced from the frequency calculations at BP86/TZVP. The Gaussian 09 program was used for all calculations.[27] The computed energetic data and the optimized Cartesian coordinates are included in the Supporting Information.

■ ASSOCIATED CONTENT

Ⓢ Supporting Information

The Supporting Information is available free of charge on the ACS Publications website at DOI: 10.1021/jacs.5b11365.

  Crystallographic information files for complex **2**. (CIF)
  Crystallographic information files for complex **3**. (CIF)
  Crystallographic information files for complex **4**. (CIF)
  Crystallographic information files for complex **5**. (CIF)
  EPR spectra, crystallographic details on complexes **2** and **4**, NMR and IR spectra, MS data, and computational details. (PDF)

■ AUTHOR INFORMATION

Corresponding Authors
*E-mail: dirk.hollmann@catalysis.de. Phone: (+49) 381 1281 352. Fax: (+49) 381 1281 51352.
*E-mail: angelika.brueckner@catalysis.de. Phone: (+49) 381 1281 244. Fax: (+49) 381 1281 51244;
*E-mail: torsten.beweries@catalysis.de. Phone: (+49) 381 1281 104. Fax: (+49) 381 1281 51104.

Notes
The authors declare no competing financial interest.

■ ACKNOWLEDGMENTS

■ REFERENCES

(1) Lewis, N. S.; Nocera, D. G. *Proc. Natl. Acad. Sci. U. S. A.* **2006**, *103*, 15729−15735.

(2) Selected recent examples: (a) Eckenhoff, W. T.; Brennessel, W. W.; Eisenberg, R. *Inorg. Chem.* **2014**, *53*, 9860−9869. (b) Zhao, J.; Minegishi, T.; Zhang, L.; Zhong, M.; Gunawan; Nakabayashi, M.; Ma, G.; Hisatomi, T.; Katayama, K.; Ikeda, S.; Shibata, N.; Yamada, T.; Domen, K. *Angew. Chem., Int. Ed.* **2014**, *53*, 11808−11812. (c) Caputo, C. A.; Gross, M. A.; Lau, V. W.; Cavazza, C.; Lotsch, B. V.; Reisner, E. *Angew. Chem., Int. Ed.* **2014**, *53*, 11538−11542. (d) Maeda, K.; Lu, D.; Domen, K. *Chem. - Eur. J.* **2013**, *19*, 4986−4991. (e) Li, C.-B.; Li, Z.-J.; Yu, S.; Wang, G.-X.; Wang, F.; Meng, Q.-Y.; Chen, B.; Feng, K.; Tung, C.-H.; Wu, L.-Z. *Energy Environ. Sci.* **2013**, *6*, 2597−2602.

(3) Chandra, A.; Uchimaru, T. *J. Phys. Chem. A* **2000**, *104*, 9244−9249.

(4) A systematic overview of possible reactions of water at a transition metal fragment was given by Piers, W. E. *Organometallics* **2011**, *30*, 13−16.

(5) Ozerov, O. V. *Chem. Soc. Rev.* **2009**, *38*, 83−88.

(6) Kohl, S. W.; Weiner, L.; Schwartsburd, L.; Konstantinovski, L.; Shimon, L. J. W.; Ben-David, Y.; Iron, M. A.; Milstein, D. *Science* **2009**, *324*, 74−77.

(7) Kunkely, H.; Vogler, A. *Angew. Chem., Int. Ed.* **2009**, *48*, 1685−1687.

(8) Kessler, M.; Hansen, S.; Hollmann, D.; Klahn, M.; Beweries, T.; Spannenberg, A.; Brückner, A.; Rosenthal, U. *Eur. J. Inorg. Chem.* **2011**, *2011*, 627−631.

(9) Hollmann, D.; Grabow, K.; Jiao, H.; Kessler, M.; Spannenberg, A.; Beweries, T.; Bentrup, U.; Brückner, A. *Chem. - Eur. J.* **2013**, *19*, 13705−13713.

(10) Kessler, M.; Schüler, S.; Hollmann, D.; Klahn, M.; Beweries, T.; Spannenberg, A.; Brückner, A.; Rosenthal, U. *Angew. Chem., Int. Ed.* **2012**, *51*, 6272−6275.

(11) Kessler, M.; Hansen, S.; Godemann, C.; Spannenberg, A.; Beweries, T. *Chem. - Eur. J.* **2013**, *19*, 6350−6357.

(12) Godemann, C.; Dura, L.; Hollmann, D.; Grabow, K.; Bentrup, U.; Jiao, H.; Schulz, A.; Bruckner, A.; Beweries, T. *Chem. Commun.* **2015**, *51*, 3065−3068.

(13) (a) Pattiasina, J. W.; Heeres, H. J.; Van Bolhuis, F.; Meetsma, A.; Teuben, J. H.; Spek, A. L. *Organometallics* **1987**, *6*, 1004−1010. (b) Horacek, M.; Gyepes, R.; Kubista, J.; Mach, K. *Inorg. Chem. Commun.* **2004**, *7*, 155−159. (c) Varga, V.; Cisarova, I.; Gyepes, R.; Horacek, M.; Kubista, J.; Mach, K. *Organometallics* **2009**, *28*, 1748−1757. (d) Gyepes, R.; Varga, V.; Horacek, M.; Kubista, J.; Pinkas, J.; Mach, K. *Organometallics* **2010**, *29*, 3780−3789.

(14) (a) Mabbs, F. E.; Collison, D. *Mol. Phys. Rep.* **1999**, *26*, 39−59. (b) Spałek, T.; Pietrzyk, P.; Sojka, Z. *J. Chem. Inf. Model.* **2005**, *45*, 18−29.

(15) Chai, J.-D.; Head-Gordon, M. *Phys. Chem. Chem. Phys.* **2008**, *10*, 6615−6620.

(16) Kumar, M.; Chaudhari, R. V.; Subramaniam, B.; Jackson, T. A. *Organometallics* **2014**, *33*, 4183−4191.

(17) Thewalt, U.; Honold, B. *J. Organomet. Chem.* **1988**, *348*, 291−303. It should be noted that the same compound was reported later to the CCDC by R. Stibrany in a private communication (2013) with Ti−O bond lengths of 2.052 and 2.053 Å.

(18) Henry-Riyad, H.; Tidwell, T. T. *J. Phys. Org. Chem.* **2003**, *16*, 559−563.

(19) Chan, K. S.; Li, X. Z.; Dzik, W. I.; de Bruin, B. *J. Am. Chem. Soc.* **2008**, *130*, 2051−2061.

(20) Bochmann, M.; Jaggar, A. J.; Wilson, L. M.; Hursthouse, M. B.; Motevalli, M. *Polyhedron* **1989**, *8*, 1838−1843.

(21) Sheldrick, G. M. *Acta Crystallogr., Sect. A: Found. Crystallogr.* **2008**, *64*, 112−122.

(22) Brandenburg, K. *DIAMOND*, version 3.2h; Crystal Impact GbR: Bonn, Germany, 2012.

(23) Perdew, J. P. *Phys. Rev. B: Condens. Matter Mater. Phys.* **1986**, *33*, 8822−8824.

(24) Schäfer, A.; Huber, C.; Ahlrichs, R. *J. Chem. Phys.* **1994**, *100*, 5829−5835.

(25) Hay, P. J.; Wadt, W. R. *J. Chem. Phys.* **1985**, *82*, 299−310.

(26) Lamac, M.; Spannenberg, A.; Baumann, W.; Jiao, H.; Fischer, C.; Hansen, S.; Arndt, P.; Rosenthal, U. *J. Am. Chem. Soc.* **2010**, *132*, 4369−4380.

(27) Frisch, M. J.; Trucks, G. W.; Schlegel, H. B.; Scuseria, G. E.; Robb, M. A.; Cheeseman, J. R.; Scalmani, G.; Barone, V.; Mennucci, B.; Petersson, G. A.; Nakatsuji, H.; Caricato, M.; Li, X.; Hratchian, H. P.; Izmaylov, A. F.; Bloino, J.; Zheng, G.; Sonnenberg, J. L.; Hada, M.; Ehara, M.; Toyota, K.; Fukuda, R.; Hasegawa, J.; Ishida, M.; Nakajima, T.; Honda, Y.; Kitao, O.; Nakai, H.; Vreven, T.; Montgomery, J. A., Jr.; Peralta, J. E.; Ogliaro, F.; Bearpark, M.; Heyd, J. J.; Brothers, E.; Kudin, K. N.; Staroverov, V. N.; Kobayashi, R.; Normand, J.; Raghavachari, K.; Rendell, A.; Burant, J. C.; Iyengar, S. S.; Tomasi, J.; Cossi, M.; Rega, N.; Millam, J. M.; Klene, M.; Knox, J. E.; Cross, J. B.; Bakken, V.; Adamo, C.; Jaramillo, J.; Gomperts, R.; Stratmann, R. E.; Yazyev, O.; Austin, A. J.; Cammi, R.; Pomelli, C.; Ochterski, J. W.; Martin, R. L.; Morokuma, K.; Zakrzewski, V. G.; Voth, G. A.; Salvador, P.; Dannenberg, J. J.; Dapprich, S.; Daniels, A. D.; Farkas, O.; Foresman, J. B.; Ortiz, J. V.; Cioslowski, J.; Fox, D. J. *Gaussian 09*, revision D.01; Gaussian, Inc.: Wallingford, CT, 2009.